Fuel 326 (2022) 125002

Contents lists available at ScienceDirect

Fuel

journal homepage: www.elsevier.com/locate/fuel

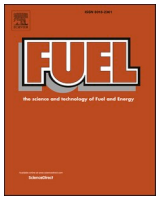

Full Length Article

Synthetic aromatic kerosene property prediction improvements with isomer specific characterization via GCxGC and vacuum ultraviolet spectroscopy

John Feldhausen, David C. Bell, Zhibin Yang, Conor Faulhaber, Randall Boehm, Joshua Heyne *

University of Dayton, Mechanical and Aerospace Engineering, Dayton, OH 45469-0238, USA

ARTICLE INFO

Keywords:
Synthetic aromatic kerosene (SAK)
Vacuum ultraviolet spectroscopy (VUV)
Property predictions
Isomer identification
Deconvolution

ABSTRACT

This research explores an advanced method of fuel composition determination and builds upon typical hydrocarbon group type analyses performed with two-dimensional gas chromatography (GCxGC). In this study, structural information of individual species within Virent's Synthetic Aromatic Kerosene (SAK) is identified by vacuum ultraviolet (VUV) spectroscopy. By mass, 71.3% of the components elute within six peaks of the chromatogram, from which 12 unique species are identified through a novel deconvolution method. Overall, the identification of 93.6%m across 26 structural isomers is made by the methods described in this work. With 93.6% m ascribed to specific isomers, the precision of fuel property predictions improves dramatically. For example, the absolute error of the viscosity prediction is reduced by 90% because of this advancement in diagnostic capability, and its 95-percentile confidence interval (precision only) is reduced by 93%. Additionally, the properties of SAK, blended with hydro processed esters fatty acids (HEFA), are demonstrated to have blended properties consistent with conventional jet fuel.

1. Introduction

The reduction of anthropogenic emissions from the transportation sector has increased interest in recent years [1]. The aviation industry consumed ~ 400 billion liters of jet fuel globally in 2019, comprising ~ 10% of greenhouse gas emissions from transportation [1–3]. Current predictions show flight demand doubling from 2010 levels by 2050 [2,4], while simultaneously, airlines continue to pledge 50% or more carbon reductions by 2050 [2]. Sustainable aviation fuels (SAFs) have been identified as the most viable option to achieve these desired carbon displacements [5] to address the rising airline industry and environmental goals.

On December 1st, 2021, a potential 100% drop-in SAF composition powered one engine on a United Airlines 737 MAX 8 flew from Chicago to Washington D.C., marking the first passenger flight powered by a potential 100% drop-in SAF [6]. The plane was propelled on a fuel blend of (1) World Energy's hydroprocessed esters fatty acids (HEFA) (ASTM D7566 A2) [7] and (2) Virent's synthetic aromatic kerosene (SAK) blended at 79 %v and 21 %v, respectively. As the name suggests, SAK is composed primarily of aromatics, which from a compositional standpoint, sharply contrasts with the composition of several other qualified SAFs. Currently, SAK is the only SAF pathway undergoing commercialization to be composed of a majority aromatic content. Aromatics are associated with higher non-volatile particulate matter (nvPM) or soot emissions, and nvPM is believed to be the primary nucleation source for aviation contrails [8]. Contrails, in turn, are suggested to be the dominant radiative forcing agent of aviation instead of CO_2 emissions alone [1]. However, not all aromatics are equivalent, with naphthalenes having higher sooting potentials [9]. Relatedly, there is broad interest in compositions within the SAF community that can remain 'drop-in' while minimizing nvPM.

Fuels are required to have 8.4%v aromatics per ASTM D7566 to remain fungible with existing aircraft and infrastructure. This requirement, among others (e.g., density), often limits the amount of SAF that can be blended with petroleum-derived Jet A because SAF historically has no aromatic content. Alternative to Jet A blending, SAK provides an entirely sustainable option to achieve the aromatics requirement. The primary concern that aromatics address is material compatibility [10,11]. Aromatics offer higher density, enabling blending with lower density fuels such as HEFA and Alcohol to Jet (ATJ) [12], and potentially a blended dielectric constant in line with conventional fuels.

* Corresponding author.

https://doi.org/10.1016/j.fuel.2022.125002
Received 22 March 2022; Received in revised form 27 May 2022; Accepted 20 June 2022
Available online 2 July 2022

Nomenclature:

A_i	area percentage of i^{th} peak per ChromSpace
A_{class}	area percentage of all peaks within a hydrocarbon group or class per ChromSpace
ASTM	ASTM International
ATJ	alcohol to jet
CI	confidence interval
FID	flame ionization detector
FTIR	Fourier transform infrared spectroscopy
GC	one-dimensional gas chromatography or gas chromatography
GCxGC	two-dimensional gas chromatography
HEFA	hydro processed esters fatty acids
LHV	lower heating value or heat of combustion
m	modulation number
MS	mass spectroscopy
n	representative (average) modulation
nvPM	non-volatile particulate matter
NIST	National Institute of Standards and Technology
NJFCP	National Jet Fuel Combustion Program
NMR	nuclear magnetic resonance
PIONA	paraffins, iso-paraffins, olefins, naphthenes, and aromatics
QSPR	quantitative structure property relationships
r^2	correlation coefficient squared
R^2	coefficient of determination
SAF	sustainable aviation fuel
SAK	synthetic aromatic kerosene
T	temperature
TSI	threshold sooting index
VUV	vacuum ultraviolet light
Y_i	mass percentage of i^{th} analyte
%m	mass percentage
%v	volume percentage
δ	fixed time interval over which absorbance was averaged
ρ	density
σ	surface tension
σ_{Y_i}	analyte quantification uncertainty
σ_z	root property data uncertainty
σ_{isomer}	isomeric uncertainty

Numerous low volume (<1mL) hydrocarbon compositional analysis methods reduce SAF scale-up risks and streamline the various qualification processes [3,13–19]. Collectively, these technologies provide fuel producers with critical property predictions that can guide feedstock-conversion engineering at earlier technology readiness levels, thereby streamlining production and investment decisions. For example, a wet waste volatile fatty production process was recently guided in part by these analyses, leading to a fuel technology readiness level in less than one year, sufficient to support ASTM D4054 testing requirements [3].

Multidimensional gas chromatography is a relatively mature technology capable of separating analytes in complex solutions and remains common in the fuel characterization community. Superposing columns with a modulator between columns affords greater separations than those afforded through single-column configurations [13,18]. Kilaz et al. provide a complete review of various analytical techniques [13], e.g., flame ionization detection (FID), mass spectroscopy (MS), Fourier transform infrared spectroscopy (FTIR), nuclear magnetic resonance (NMR), and concluded that multidimensional chromatography offers the highest R^2 for property relationship modeling. These GC × GC configurations require 'stencil' calibration using MS results and reference samples. Once calibrated, stencils can determine the boundaries of various hydrocarbon classes and carbon numbers [20]. However, even when coupled with MS detectors, stencil techniques cannot determine structural differences between most isomers [13]. VUV offers structural information; therefore, it has gained popularity in the food, forensics, environmental, and fuel research communities [18,21–24]. Gas chromatography techniques with VUV analysis have demonstrated the capability to identify structural and stereoisomers such as p-xylene, o-xylene, m-xylene [21], or the isomers of *cis*-decalin and *trans*-decalin [18], which have been indistinguishable by MS systems.

Schug et al. explored the benchtop VUV detector in 2014 [21], suggesting its potential as a universal detector. Select species, separated from a gasoline sample, were resolved at the isomeric level in that work [21]. A later publication by Walsh et al. demonstrated the use of GC-VUV for hydrocarbon group type analysis (PIONA) of gasoline which was verified through various existing ASTM compositional methods [25]. However, in the case of a higher molecular weight jet fuel such as SAK, with higher isomerization, the second chromatographic dimension is necessary to separate analytes sufficiently. More recently, Wang explored a diesel fuel sample in a GCxGC-VUV configuration. Still, similar to Walsh et al. [25], the work was only concerned with group type analysis between cycloalkanes and alkenes rather than specific isomeric structures [26].

Property predictions from the compositional analysis have long been of interest within the fuel community [13,14,18,27]. Before Yang et al. [16], most fuel property predictions could be classified as 'top-down' approaches [19,28], where models are developed by regression of measured data, serving as both the independent and dependent variables. Such models risk extrapolating to non-physical results (regardless of the statistical method) and require substantial data to quantify uncertainties [18]. Conversely, 'bottom-up' approaches [16,18,29] leverage composition data via GCxGC as one category of input and a library of property data corresponding to potential fuel constituents like the other category of input. These inputs are related to fuel properties, usually by physically based, verified blending rules [16–18,30]. While the blending rules afford confidence to extrapolate to compositions beyond the historical record, all such bottom-up models afford traceability of errors, enabling a comprehensive uncertainty analysis [17,18]. The four sources of error that contribute to the uncertainty of predictions made by a bottom-up approach include the following: constituent mass concentration measurement error from a chromatogram peak (possibly deconvoluted), assignment of chromatogram peaks to specific isomers, isomeric properties data uncertainty, and blending rule accuracy. This work addresses the precision of the chromatogram peak assignments to specific isomers, as well as the identification and deconvolution of chromatogram peaks comprised of up to 3 species.

A contemporary SAF candidate (Virent SAK) is investigated with no prior knowledge of composition or properties, starting with GCxGC-FID/VUV. Much of its composition (>71 %m) is found in coeluting peaks. Here, an isomeric identification approach is detailed with four novel contributions: (1) definitive determination of species count (one or more than one) within any peak on the chromatogram, (2) two-dimensional VUV deconvolution with up to three analytes, (3) greater than 93%m in a jet fuel is assigned to 26 specific isomers, and (4) precision improvement of property predictions. Previous coelution detection methodologies leverage the completeness of reference libraries [25,26], whereas the method presented here relies solely on the measured signal. This definitive pre-processing of peaks distinguishes single elution from coelution peaks and categorizes them based on the presence of multiple unique spectra within the same peak. Finally, material compatibility and dielectric constant calculations are reported for 79/21 %v HEFA/SAK blend, further documenting the potential of SAK as a keystone blend

component for potential 100% SAF.

2. Methodology

A GC × GC-FID/VUV method was employed to identify the hydrocarbon species in SAK, similar to the method used in Heyne et al. [18]. This work builds on that methodology by adding deconvolution capabilities, dramatically reducing predictive uncertainty due to isomeric information, and compares them to predictions done with traditional hydrocarbon group type information [16].

2.1. Reference samples

The SAK fuel sample was provided courtesy of Virent, Inc, and the HEFA fuel sample was provided by World Energy. Additional materials that composed the majority of the SAK were procured to predict SAK properties more accurately and characterize the mixture further. A summary of measured properties for each component can be found in Tables 2 and 3 in the Supplementary Material. Three reference fuels from the National Jet Fuel Combustion Program (NJFCP) [27,31,32], A-1 (POSF 10264), A-2 (POSF 10325), and A-3 (POSF 10289), were also analyzed via GC × GC-FID/MS and used as an aromatic benchmark for several temperature-independent properties.

2.2. Gas chromatography, flame ionization detector, and vacuum ultraviolet light detector

The experimental setup was arranged as GCxGC-FID/VUV, where the VUV system supported the hydrocarbon isomeric identification and the FID supported quantification. The system included two columns separated by a modulator connected to a split plate after the second column, where the analytes were directed to either the FID or the VUV. The system included a SepSolve INSIGHT flow modulator and VGA-101 Vacuum Ultraviolet light detector. A graphical overview of the GCxGC-FID/VUV is displayed in Fig. 1, illustrating the major components of the GCxGC-FID/VUV system.

The Agilent 7693A Automatic Liquid Sampler (ALS) injected 5 μ L of sample into the Agilent 8890 GC. The inlet temperature, pressure, and split ratio were maintained at 250 °C, 55.04 psi, and 100:1, respectively. A reverse column arrangement was chosen to achieve the desired separations for this study. Specifically, in their respective order, a Rxi-17Sil MS 60 m × 0.32 mm × 0.5 µm and Rxi-1 15 ms × 0.32 mm × 0.5 µm columns were utilized, both of which were manufactured by Restek. Constant flow rates for the first and second columns of 1.2 mL/min and 48 mL/min were held throughout the run with a Helium carrier gas (grade 5.0), which passed through a Restek Triple Filter before entering the GC system. The GC oven was initialized at a temperature of 40 °C for 30 s, with a ramp rate of 1 °C / min until achieving a final temperature of 280 °C, where the temperature was held for 10 min. The GC ran for a total time of 250.5 min. Two modulation times and injection volumes were used. A 10-second modulation time with 5 μ L injection and a 5-second modulation time with 1 μ L injection was employed. The combination of long modulation times and high injection volumes enabled higher concentrations of trace analytes to be identified. In comparison, the shorter modulation time and lower injection volume facilitated deconvolution of peaks with high concentrations.

As mentioned previously and demonstrated in Fig. 1, the analyte is divided at the split plate after traveling through the secondary column. One of the lines leaving the split plate junction feeds the FID, where flow rates are applied to the air (ultra-zero grade) flow, H_2 (grade 6.0), and N_2 (grade 5.0) at flow rates of 400, 40, and 25 mL/min, respectively. The FID operated at a fixed temperature of 300 °C while recording data at a frequency of 50 Hz, which was processed by INSIGHT ChromSpace software (Version 1.5.1).

As illustrated in Fig. 1, a second line parts from the split plate and directly connects to the VGA-101 transfer line. The sample was preferentially directed to the VUV detector relative to the FID. The length of the internal transfer line from the split plate to the VUV was shorter than the transfer line from the split plate to the FID to increase the amount of sample directed to the VUV. The transfer line from the GC to the flow cell was maintained at 250 °C. With N_2 (grade 5.0) being used as the system gas, data acquisition continuously occurred at 76.92 Hz over a wavelength range of 125 to 430 nm.

2.3. Identification and Quantification:

The overall identification procedure includes the following steps: timestamp alignment between FID and VUV, removal of oversaturated VUV data, local background signal subtraction and noise reductions, coelution screening, identification of analyte(s) in the considered peak, and conversion to mass fractions. Each step of the procedure described above leveraged in-house Python (Version 3.8.5) code.

2.4. FID and VUV alignment

Synchronization of the FID signal to the VUV signal was completed by aligning the max signal for each peak across the experiment duration. A single offset value could be found and applied to the entire VUV dataset by minimizing the offset between the local maxima found with the separate detectors. With the offset applied, SepSolve ChromSpace FID area determinations were associated with the identified analytes and VUV data.

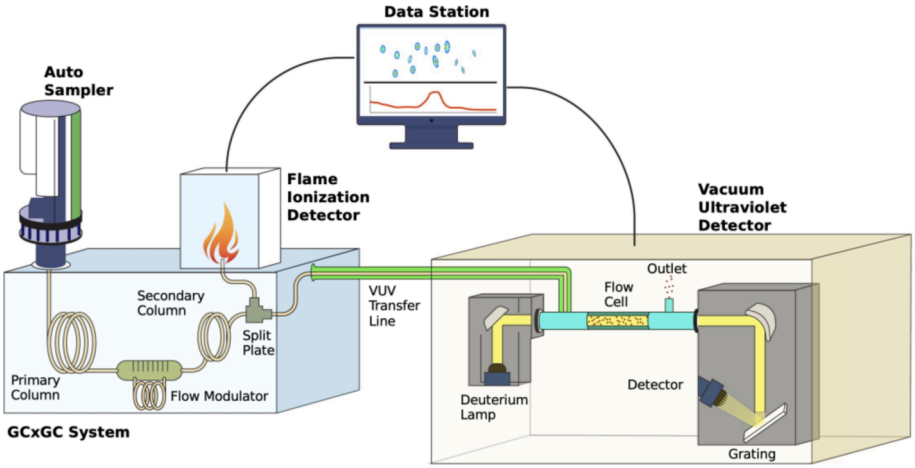

Fig. 1. GC × GC-FID/VUV Test Setup Diagram.

2.5. Analyte identification

Pre-processing of VUV spectra included screening for oversaturation. Then local background subtraction and signal averaging, akin to the approach described in Lelevic et al. [33] and Heyne et al. [18], were done to attain the sample spectra used for matching against cataloged reference spectra. Single analyte identification followed the work discussed in Heyne et al. [18].

Determination of species count (one or more than one) within each peak on the chromatogram was the final pre-processing step. Prior state-of-the-art techniques [25] relied on the quality (e.g., R^2) of a multiple species match significantly exceeding that of the top single species matches to confirm or reject the presence of coelution. This work shows how this determination can be established prior to any matching exercise, eliminating reliance on spectral reference libraries' completeness. This insight is instrumental in downstream steps. For example, by demonstrating that given sample spectra originates from a single species, subsequent comparison to reference spectra will either identify the most probable match or prove that the observed sample spectra are not present in the reference library. Without first proving that sample spectra originated from a single species, any number of linear combinations of multiple spectra in the reference library could (incorrectly) meet the acceptable match criteria. Conceptually, the coelution check is done by comparing sets of spectra that are each averaged over the full width of one retention time axis (i.e., t_1 or t_2) and segments of the other retention time axis. If the spectral profile is static while sweeping through the segmented time axis, in both dimensions, the peak is comprised of a single analyte. If the normalized spectra change while traveling across the chromatogram peak, it is known to be comprised of multiple analytes.

For chromatogram peaks consisting of more than one species, the sample VUV spectra at each point in time (t_1, t_2) within that peak were matched by a linear combination of 2 or 3 reference spectra, leveraging the non-negative least-squares optimization algorithm from Python SciPy, maximizing R^2. The decision logic around which 2 or 3 reference spectra to use as the basis functions was partially manual, with the goal being to select the ones that yielded the best overall match throughout the peak. The overall concentration of each analyte was determined by summing the product of the reference spectra scale factors at each time point with the mass fraction attributed to each time point, where the integrated areas of sample VUV spectra were used to determine the mass fraction at each time point.

2.6. Quantification

Hydrocarbon type analysis was performed by generating a stencil with a method like the one described by Vozka et al. [34]. Chromatogram peak areas of each peak (A_i) were determined through the ChromSpace integration software and attributed to corresponding hydrocarbon groups (A_{class}) based on retention time, where the FID signal serves as the z-axis (or the color scale). Previous research [16–18] has leveraged the well tested template from Striebich et al. for hydrocarbon group type mass fraction determinations [20], as were the mass fractions (Y_i) presented herein. To arrive at a single species mass fraction, the group mass fraction per the Striebich et al. template (Y_{class}) was scaled by the area percentage of the selected peak (A_i) relative to the total area (A_{class}) of the respective hydrocarbon group. Repeatability for hydrocarbon class quantification is taken as RSD% <1.5% (n = 3), as reported in a recent repeatability study [35].

$$Y_i = \frac{A_i}{A_{class}} * Y_{class}$$

2.7. Property measurements

Threshold Sooting Index (TSI) values of each species identified in the report were estimated via the QSPR model of Boehm et al. [9], and the blending rule detailed in that report was used to predict the TSI of SAK. An o-ring volumetric swell study was performed with optical dilatometry techniques described in Faulhaber et al. [36]. Here, two acrylonitrile-butadiene o-ring materials were submerged at room temperature into separate fuel-filled vials. The first contained neat HEFA, and the second had a 79/21 %v HEFA/SAK blend. Refractive index measurements were taken at room temperature using a Reichert TS Meter. These measurements were taken with a light emission source at 589 nm and converted into dielectric constant values for neat HEFA, SAK, and the 79/21 %v HEFA/SAK using $K = n^2$ (K is dielectric constant, n is refractive index). The accuracy of the Reichert TS Meter was +-0.0001 nD. Other properties such as flash point, freeze point, viscosity, density, and surface tension, were experimentally determined for several samples using aviation fuel specification tests [7]. Both the ASTM methods' names and corresponding repeatabilities and reproducibilities are listed in Table 1 of the Supplementary Material and serve to evaluate the accuracy of the predictions. [9]. All other properties required but not measured for this study were sourced by the NIST Web Thermo Tables [37].

2.8. Tier Alpha approach for property predictions

The Tier Alpha approach for property predictions employs three different pieces of information: empirically derived algebraic blending rules, an extensive database of pure molecules, and the best available composition data. Where composition data is limited to hydrocarbon group level mass concentrations, a random selection of a representative member of that group is made as part of a Monte Carlo simulation that also includes uncertainties in determining mass fractions and database properties. By far, the largest source of uncertainty (precision) in these determinations has been, until recently [18], the underdetermined speciation within each of the hydrocarbon groups [17]. The coupling of VUV spectroscopy with GCxGC-FID chromatography addresses this primary source of property prediction uncertainty, and now, with this work, advances in sampled VUV spectra deconvolution further attack this primary source of property prediction uncertainty. With these

Table 1
Summary of the identification results organized by hydrocarbon groups. Identified species are listed along with their corresponding chromatograph peak labels in Fig. 3.

Group Type	Species Name	Labels	%Mass
C9 Cycloaromatics	indane	p	0.799
C8 Alkylbenzenes	p-xylene	b*	0.384
	m-xylene	b*	1.274
	ethylbenzene	a	0.181
	o-xylene	c	1.844
C9 Alkylbenzenes	1-methyl-3-ethylbenzene	f*	20.604
	1-methyl-4-ethylbenzene	f*	10.879
	1,3,5-trimethylbenzene	f*	0.148
	1,2,4-trimethylbenzene	h*	26.686
	Isopropyl benzene	d	0.275
	n-propylbenzene	e	1.92
	1-methyl-2-ethylbenzene	g	1.356
	1,2,3-trimethylbenzene	l	0.163
C10 Alkylbenzenes	*sec*-butylbenzene	i*	0.156
	1,3-diethylbenzene	m*	4.445
	1-methyl-3-n-propylbenzene	m*	3.213
	1-methyl-4-n-propylbenzene	m*	1.535
	1,3-dimethyl-5-ethylbenzene	n*	1.122
	1,4-diethylbenzene	n*	0.811
	1-methyl-3-isopropylbenzene	j	0.739
	1-methyl-4-isopropylbenzene	k	0.332
	1-methyl-2-n-propylbenzene	o	0.145
	1,4-dimethyl-2-ethylbenzene	q	0.678
	1,3-dimethyl-4-ethylbenzene	r	2.443
	1,2-dimethyl-4-ethylbenzene	s	10.089
	1,2,4,5-tetramethylbenzene	t	1.36

improvements, blending rule accuracy, rather than prediction precision, maybe the largest source of overall prediction uncertainty for some properties of some hydrocarbon mixtures with volatility within the jet fuel range. A flow chart describing this process is provided in Fig. 2 to help conceptualize the details of this approach.

3. Results and discussion

3.1. Identification results

The hydrocarbon group type analysis from the GCxGC chromatograph template classifies 93.2 %m into three alkylbenzene bins; C8 (3.7%m), C9 (62.0 %m), and C10 alkylbenzenes (27.5%m). Other minor fractions are distributed across C9 (0.8 %m) and C10 cycloaromatics (1.2 %m), along with various cycloalkane and *iso*-alkane groups, each < 1.5%m, across a carbon range of C8 to C10. While that approach classifies analytes into a specific hydrocarbon group, this study aims to further separate the group mass fraction into isomer-specific fractions using VUV data. Illustrated in Fig. 3, the SAK chromatograph has been labeled with English letters to inform which peaks were identified using the VUV detector. These English letters, summarized in Table 1, delineate 26 isomers along with their mass fractions amounting to 93.6 %m of the SAK sample. All possible isomers of C8 and C9 alkylbenzenes are identified. In contrast, C9 cycloaromatics and C10 alkylbenzenes include incomplete isomer identification due to some peaks having a low signal to noise or due to detected isomers not matching against the available reference data. All fractions from the hydrocarbon group type analysis that were not identified on the isomeric level have been summarized in Table 4 of the Supplementary Material.

The two most prominent analytes present in SAK are 1-methyl-3-ethylbenzene and 1,2,4-trimethylbenzene, 20.6%m and 26.7 %m, respectively. Conversely, 1-methyl 2-n-propyl benzene (0.15 %m) and 1,3,5-trimethylbenzene (0.15 %m) are the smallest identifiable fractions. All peaks comprising at least 0.68%m of the SAK sample were identified by matching their corresponding VUV spectra with reference spectra in our library; R^2 greater than 0.999. At lower analyte concentration, the R^2 between sample and reference spectra of the same species decreases due to the low signal-to-noise ratio of the sample spectra. For 1-methyl 2-propylbenzene, the R^2 was 0.978.

The VUV performed excellently in the hydrocarbon group regions where the reference library was completely defined for all isomers in that hydrocarbon class and carbon number. Conversely, limitations persist in identifying analytes in regions with poor or incomplete library spectra. This is especially true in higher SAK MW regions (>C10), where known possible isomers exponentially increase. For example, two prominent cycloaromatic peaks (lower right diagonal of the chromatogram peak 's,' Fig. 3) are not identified beyond the hydrocarbon group type analysis. Conversely, all C8, C9, and C10 alkylbenzene isomer spectra are present within the reference library, enabling comprehensive identifications. Additionally, as demonstrated by Lelevic et al., lower carbon number alkylbenzenes exhibit higher absorption (higher response factor) relative to other hydrocarbon class species. Alkanes, in contrast with low molecular weight alkyl benzenes, require higher molar concentrations for equivalent identification fidelity [38].

3.2. Two-Dimensional deconvolution

Paramount to the success of identifying isomers in SAK is deconvolution capability. Coeluting species are marked with an asterisk (*) next to their peak letter label in Table 1. Collectively, 71.3 %m is contained in 6 peaks that required deconvolution, while 22.3 %m contained in 14 peaks did not require deconvolution. Nearly half of the identified isomers in this analysis required deconvolution for identification.

Fig. 4 illustrates the deconvolution analysis of the most prominent peak in the SAK sample (labeled 'f*' in Table 1 and 'f' in Fig. 3). The bulk mass fraction of the peak is determined to be 31.6 %m of the total SAK composition. Namely, 1-methyl-3-ethylbenzene, 1-methyl-4-ethylbenzene, and 1,3,5-trimethylbenzene are found in this peak. The majority of this peak (99.54%m) is comprised of 1-methyl-3-ethylbenzene and 1-methyl-4-ethylbenzene. Also, 1,3,5-trimethylbenzene is found in low concentrations here, 0.15%m total SAK mass or 0.46%m of the peak, respectively. Linear combinations of the scaled reference spectra for the three analytes of interest here achieve an R^2 greater than 0.999 at each timestamp reported.

The analytes at peak 'f' in Fig. 3 exhibit a saturated VUV signal (absorbance exceeding 1.0) at some wavelengths, making its deconvolution less rigorous. To avoid that complication, the reduced injection volume method as described in the method section was applied. Fig. 4 illustrates a blow-up of this peak after applying the reduced injection volume method. In contrast to Fig. 3, the image shown in Fig. 4c is from the VUV signal rather than the FID signal.

Fig. 4a and 4d report the relative absorbance of 1-methyl-3-ethylbenzene and 1-methyl-4-ethylbenzene. Mathematically the absorbance signatures are dramatically different and distinguishable. The first

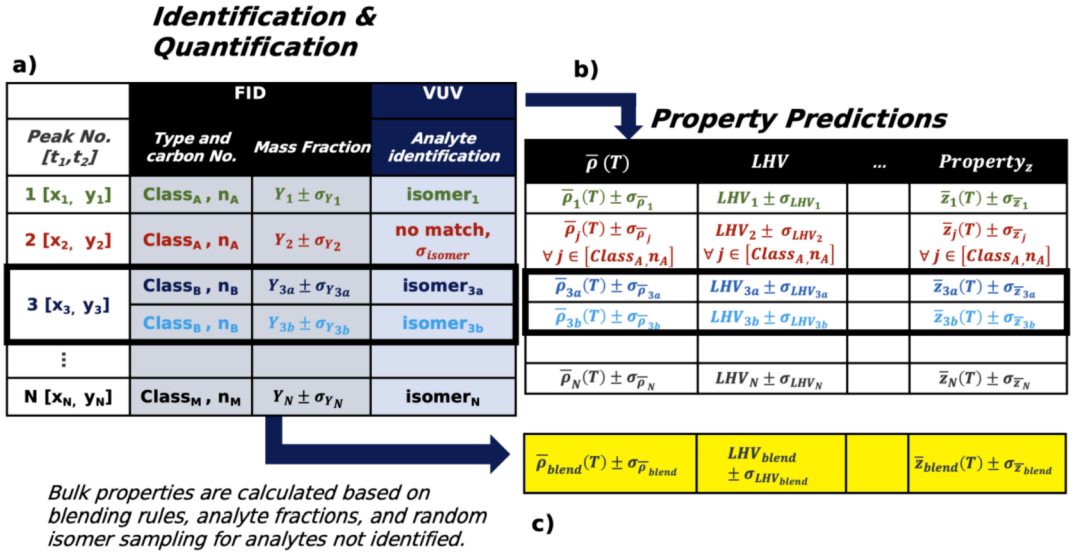

Fig. 2. Illustration of the 'Tier Alpha' approach, including identification and quantification (a), component property data (b), and mixture property determinations (c). Deconvolution is depicted with a bold black outlined box.

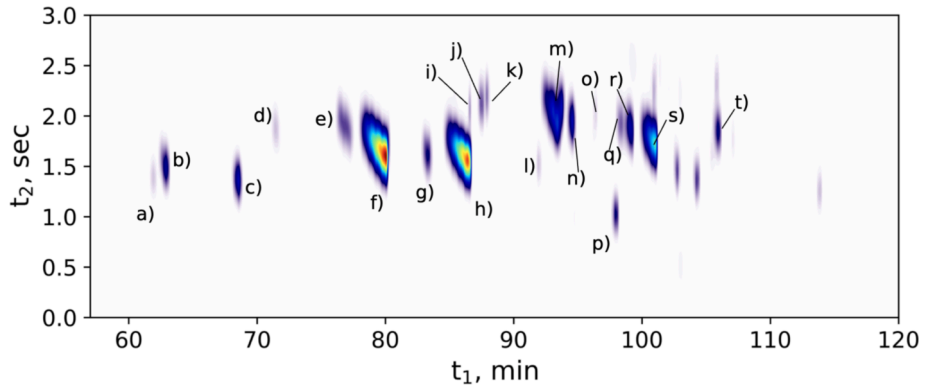

Fig. 3. FID chromatograph (5 μ L and 10 sec modulation time) with provided letters that correspond to identified species laid out in Table 1. The RGB color scheme is used where blue is low signal intensity (or concentration), and red is high signal intensity (or concentration). (For interpretation of the references to color in this figure legend, the reader is referred to the web version of this article.)

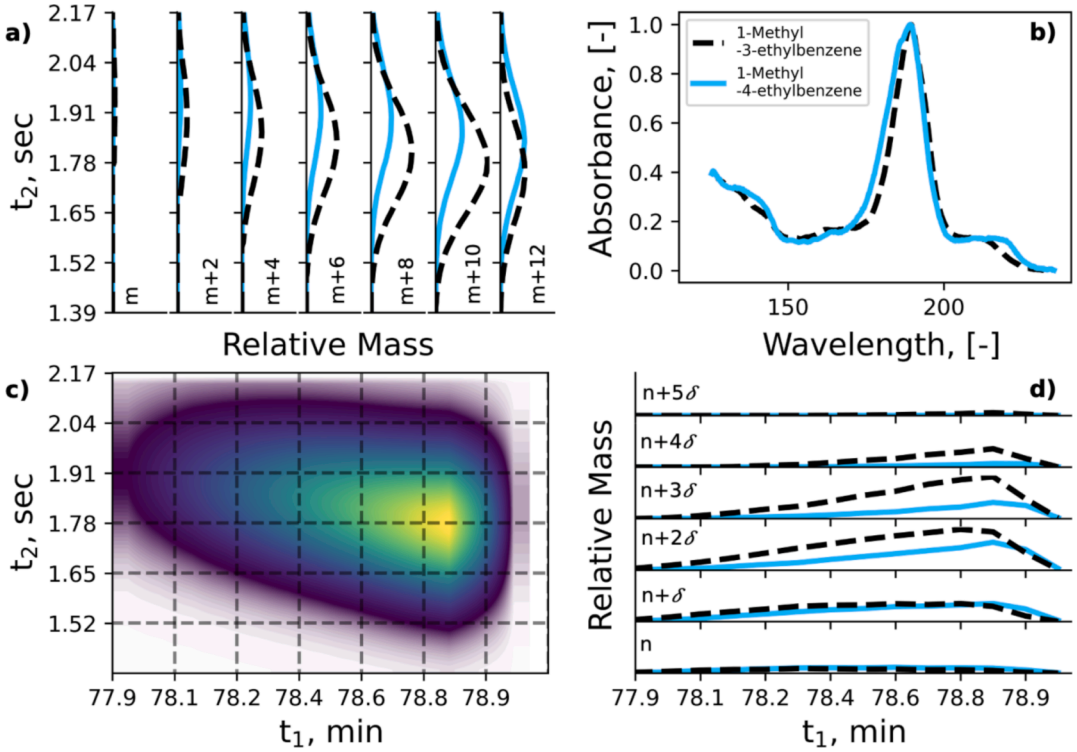

Fig. 4. An illustration of the relative masses across peak 'f' (Fig. 3), determined through two-dimensional deconvolution (a and d) of 1-methyl-3-ethylbenzene (dashed black line) and 1-methyl-4-ethylbenzene (solid blue line). Subplots (c and d) depict the integrated VUV signal as a chromatographic peak and the normalized reference spectra of each species, respectively. (For interpretation of the references to color in this figure legend, the reader is referred to the web version of this article.)

dimension of separation, t_1, is the recorded time corresponding to the modulation number, '*m*,' at a given analyte entered the secondary column. The second dimension, t_2, corresponds to the detection time in the VUV for a given modulation. Fig. 4a illustrates the relative mass fractions of 1-methyl-3-ethylbenzene (dashed black lines) and 1-methyl-4-ethylbenzene (solid blue lines) over a given modulation index ('*m*'). Fig. 4d compares the relative mass fractions of 1-methyl-3-ethylbenzene and 1-methyl-4-ethylbenzene for selected bins of t_2 values, with '*n*' representing the first bin, and δ representing the width of each bin over t_2 for which absorbance was averaged. By parsing out the concentrations of each analyte across all of the peak timesteps, the accuracy of the aggregate concentrations (across the whole peak) improves. Furthermore, it is possible to detect the presence of minor peak concentrations, that are otherwise unidentifiable if looking at the average signal or summed signal of the entire peak, e.g., this deconvolution method reveals the presence of 1,3,5-trimethylbenzene at the low concentration of 0.15 %m.

3.3. Fuel properties

Two sets of predictions, derived from our 'Tier Alpha' [16] methodology, are made and compared with laboratory measurements. In one set of predictions ('Tier Alpha + VUV'), the information conveyed in Table 1 is utilized in the calculations. For the other set of predictions ('Tier Alpha'), the total mass fraction of each hydrocarbon group type is randomly assigned to a specific isomer of the group in a Monte Carlo simulation. Either way, the properties of each specific component in the mixture-as-modeled are necessary input. The following mixture

properties were measured and/or predicted in this work: surface tension at 22 °C, lower heating value (LHV), flash point, threshold sooting index (TSI), smoke point, freeze point, density as a function of temperature, and viscosity as a function of temperature, seal swell, and dielectric constant at 22 °C.

Several temperature-independent property results are presented in Fig. 5. Measurement data is represented by black-filled circles and lines. Predictions without (Table 1) isomer specificity are represented by blue open triangles and lines. Predictions that leverage the data presented in Table 1 are represented by red open circles and lines. Uncertainties for each determination are represented with 68 % confidence intervals (CI), solid lines, and 95 % CI, capped dashed lines. The accuracy of the applicable blending rule is not captured in the displayed confidence intervals. The green shaded region is derived from the aromatic fraction of the three reference fuels from the NJFCP: A-1 (POSF 10264), A-2 (POSF 10325), A-3 (POSF 10289). They are each the union of three 95% CIs as determined by the 'Tier Alpha' predictions, and the green regions are intended to provide an additional context of where property values typically lie for the aromatic fraction of conventional fuels.

As evident in Fig. 5, the confidence intervals (precision) of the predictions are markedly decreased when 93.6%m is attributable to specific isomers, which is not surprising since isomer uncertainty has been previously identified as the leading source of uncertainty in 'Tier Alpha' predictions when mass concentrations are lumped by hydrocarbon group [17,18]. With the improved prediction precision via specific isomer identifications, the prediction accuracy can be assessed more clearly. In these examples, however, the confidence intervals of the measurement overlap with those of both sets of predictions. Essentially no change in prediction accuracy is observed. The small shift in the prediction mean of LHV is consistent with the expectation that actual population distributions of isomers within any given hydrocarbon group

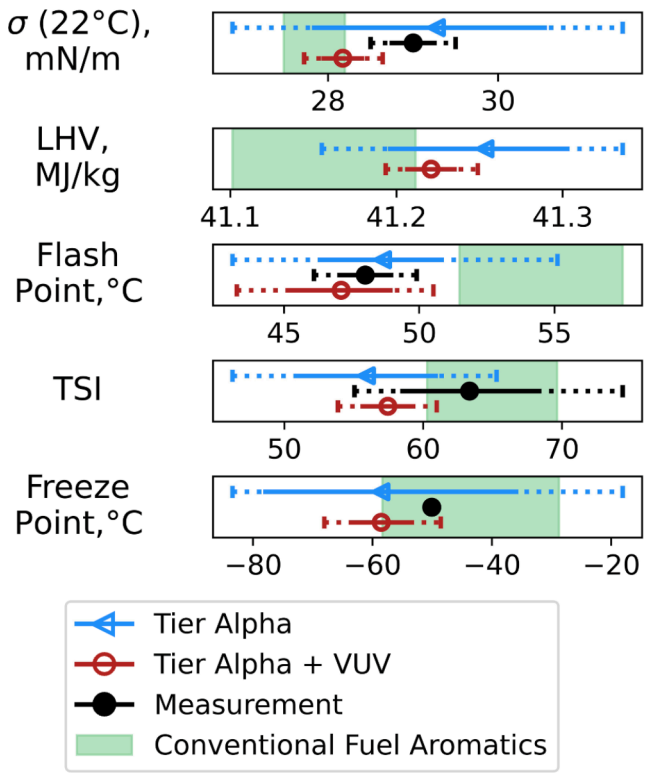

Fig. 5. Comparison of predictions of 'Tier Alpha' (blue symbols and lines) to 'Tier Alpha + VUV' (red symbols and lines) in relation to nominal values determined through direct property measurement under ASTM standard methods. Conventional fuel (Jet A - only aromatic components) 95 % CI plotted as well in light green for reference. (For interpretation of the references to color in this figure legend, the reader is referred to the web version of this article.)

are skewed toward lower heats of formation, not uniform [17]. The larger shift in the prediction mean of surface tension (σ) as well as the 4-5x improvement in the prediction precision underscores the value of the greater specificity of species identification afforded by the GCxGC-FID/VUV method relative to other separation methods where the analytes cannot be interrogated by a spectrographic method, such as VUV. The offset between the two mean surface tension predictions is due largely to the difference between the actual population distribution of C9 alkylbenzenes (accounting for 62.02 %m of the sample SAK) relative to a presumed uniform population distribution of these isomers. The mass fraction weighted average surface tension of the C9 alkylbenzenes is 0.9 mN/m less than the average surface tension of the C9 alkylbenzenes bin.

Viscosities and densities for SAK are illustrated in Fig. 6 over a temperature range important to the safe operation of jet engines [27]. Specifically, Fig. 6 includes SAK measurements, black circles, 'Tier Alpha' predictions without Table 1 inputs (blue lines), and 'Tier Alpha + VUV' predictions with Table 1 inputs (red lines). Uncertainty regions for each of the predicted methods are also included, where the light regions represent the 95% CIs, and the darker shaded regions represent the 68 % CIs. Device-reported uncertainties are also reported with error bars but are mostly masked due to scaling. Viscosity predictions, with Table 1 inputs, outperformed the standard 'Tier Alpha' by achieving reductions of 90% and 93% for mean error and 95 % CI, respectively. For density, mean error and 95 % CI reductions of 75 % and 89 % are observed, respectively. These accuracy and precision improvements are credited to the removal of the isomeric uncertainty gained by identifying the specific isomers that comprise more than 93%m of the SAK sample. The tier alpha method with either set of inputs, applied to viscosity, demonstrates better agreement with experimental data between 0 °C and 20 °C than they do below 0 °C. For viscosity, a portion of the error at the lower temperatures is due to error imparted through extrapolation (ASTM D341)[39] to lower temperatures than those available through NIST Thermo Tables [38]. This decrease in predictive accuracy between 0 °C and 20 °C was also observed in Heyne et al. [18]. The temperature sensitivity of density ($\Delta\rho/\Delta T$) is well captured by 'Tier Alpha + VUV' (with Table 1 inputs); deviating from the data by just 0.39%. A full tabulation of the neat material property measurements is available in Tables 2 and 3 of the Supplementary Material.

High carbon balance can be achieved with the techniques described in Section 2. The VUV absorption spectra for all known structural isomers of the major aromatic regions in this study (C8, C9, and C10 alkylbenzenes) were fully catalogued in our reference spectra library, thus eliminating concerns of encountering a false-positive match. Generally, as reference libraries become more complete at higher carbon numbers and other hydrocarbon types, the analysis demonstrated here will illuminate even more complicated and heavier fuels. To date, however, incomplete spectra libraries are relevant in instances of higher carbon numbers. For example, the two peaks to the lower right of 1,2-dimethyl-4-ethylbenzene (peak 's') in Fig. 3 are unable to be resolved, likely due to incompletely catalogued VUV reference spectra for C10 cycloaromatics.

3.4. HEFA/SAK blend and HEFA properties

As mentioned in the introduction, aromatics facilitate compliance with several key properties, including material compatibility and dielectric constant. Compositions that are non-compliant with these two additional constraints, or any other fit-for-purpose or spec'd property (ASTM D7566), are not viable candidates for a 100% synthetic SAFs. Fig. 7 reports the o-ring swelling, calculated dielectric constant values, and other important operability properties for a 79/21 %v HEFA/SAK blend and neat HEFA and neat SAK where available. Consistent with previous plots, the measurements (filled symbols) and uncertainties (error bars) are reported. These values are compared against a conventional fuel range (shaded green) and the specification limits (red lines and shaded regions) described in ASTM D7566 [7]. The blended

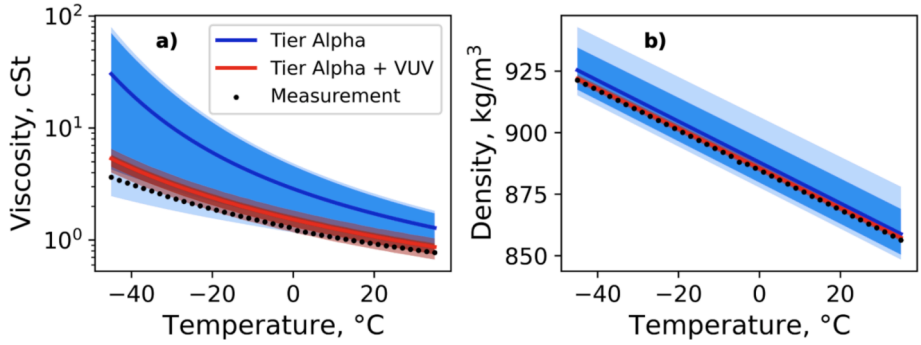

Fig. 6. Predictions of viscosity and density with respect to temperature for Tier Alpha (blue line and shaded region) and Tier Alpha + VUV predictions (red line and shaded regions) in relation to measurement (black data points). (For interpretation of the references to color in this figure legend, the reader is referred to the web version of this article.)

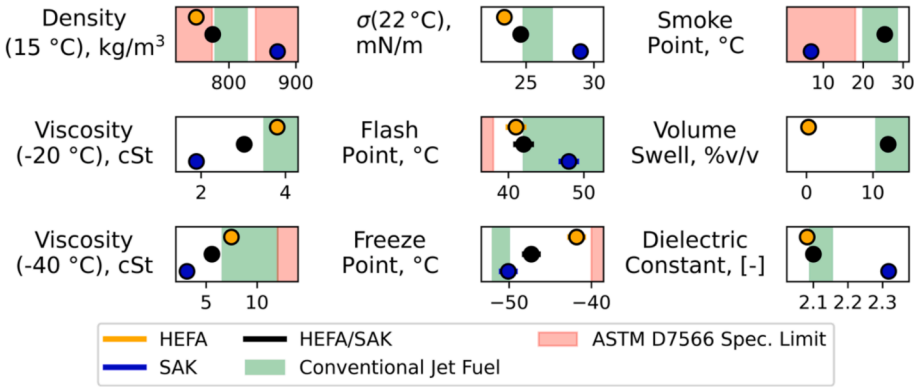

Fig. 7. Selected 'fit for purpose' operability property measurements (black symbols) with measurement error (black lines), along with o-ring volume swell percentage and dielectric constant for 79/21 HEFA/SAK blend. Neat HEFA (yellow symbol and line) and neat SAK (blue symbol and line) are plotted. Conventional Jet Fuel (shaded green) and ASTM D7566 (shaded red) illustrate compliance. (For interpretation of the references to color in this figure legend, the reader is referred to the web version of this article.)

HEFA/SAK composition is within the observed range of conventional fuels for each property considered in this work. Interestingly, the viscosity of the HEFA/SAK blend is significantly lower than the typical viscosities of conventional fuels. This is advantageous to engine operability as low viscosity often leads to finer and more uniformly distributed sprays at engine operating conditions that are consistent with altitude relight, ground start, and transitions in or out of flight idle [40,41]. Specifically, both the volume swell (12.3%) and predicted dielectric constant (2.096) are within the conventional fuel range.

4. Conclusions

A carbon balance greater than 93%m consisting of 26 separate analytes was identified in a relevant SAF (SAK) candidate. Of these, 73.1%m relied on the deconvolution method described herein. With added specific isomeric information, confidence in the property predictions improves relative to predictions predicated on conventional hydrocarbon group type analysis. Most notable, viscosity absolute error is reduced by 90% and 95-percentile confidence interval is reduced by 93%. For the properties measured, a HEFA/SAK blend illustrates a path for 100% SAF to remain drop-in for additional aviation properties (o-ring swelling and dielectric constant), while reducing nvPM with high relative aromatic contents and exhibiting other advantaged properties. Approximately 50%m of a typical conventional Jet-A is composed of in 44 peaks, meaning the limit of detection for a VUV is not the limiting factor in using it for property evaluations. While the number of analyte spectra is the limiting bottleneck in GCxGC-VUV to property predictions, the potential for this method remains exceptionally high.

Funding

The authors would like to acknowledge funding from the U.S. Federal Aviation Administration Office of Environment and Energy through ASCENT, the FAA Center of Excellence for Alternative Jet Fuels and the Environment, project 65 through FAA Award Number 13-CAJFE-UD- 026 (PI: Dr. Joshua Heyne) under the supervision of Dr. Anna Oldani. Any opinions, findings, conclusions, or recommendations expressed in this material are those of the authors and do not necessarily reflect the views of the FAA or other sponsors. Additional support for this paper was provided by US DOE BETO through subcontract PO 2196073.

CRediT authorship contribution statement

John Feldhausen: Conceptualization, Methodology, Software, Formal analysis, Investigation, Resources, Data curation, Visualization, Validation, Writing - original draft, Writing – review & editing. **David C. Bell:** Conceptualization, Methodology, Software, Formal analysis, Investigation, Resources, Data curation, Validation, Writing – review & editing. **Zhibin Yang:** Formal analysis, Investigation, Data curation, Visualization, Writing – review & editing. **Conor Faulhaber:** Investigation, Data curation, Writing – review & editing. **Randall Boehm:** Formal analysis, Writing – review & editing. **Joshua Heyne:** Conceptualization, Methodology, Supervision, Funding acquisition, Investigation, Writing – review & editing.

Declaration of Competing Interest

The authors declare that they have no known competing financial interests or personal relationships that could have appeared to influence the work reported in this paper.

Appendix A. Supplementary data

Supplementary data to this article can be found online at https://doi.org/10.1016/j.fuel.2022.125002.

References

[1] Lee DS, Fahey DW, Skowron A, Allen MR, Burkhardt U, Chen Q, et al. The contribution of global aviation to anthropogenic climate forcing for 2000 to 2018. Atmospheric Environment 2021;244. 10.1016/j.atmosenv.2020.117834.

[2] Vardon DR, Sherbacow BJ, Guan K, Heyne JS, Abdullah Z. Realizing, "net-zero-carbon" sustainable aviation fuel. Joule 2022;6:16–21. https://doi.org/10.1016/j.joule.2021.12.013.

[3] Huq NA, Hafenstine GR, Huo X, Nguyen H, Tifft SM, Conklin DR, et al. Toward net-zero sustainable aviation fuel with wet waste–derived volatile fatty acids. Proc Natl Acad Sci U S A 2021;118(13). https://doi.org/10.1073/PNAS.2023008118/-/DCSUPPLEMENTAL.

[4] U.S. Energy Information Administration. Annual Energy Outlook 2021 2021. https:// www.eia.gov/outlooks/aeo/. (accessed January 26, 2022).

[5] de Jong S, Antonissen K, Hoefnagels R, Lonza L, Wang M, Faaij A, et al. Life-cycle analysis of greenhouse gas emissions from renewable jet fuel production. Biotechnol Biofuels 2017;10:1–18. https://doi.org/10.1186/S13068-017-0739-7/TABLES/4.

[6] World's first passenger flight with 100% renewable fuel takes off—thanks to biotech | BIO n.d. https://www.bio.org/blogs/worlds-first-passenger-flight-100-renewable-fuel-takes-thanks-biotech (accessed May 9, 2022).

[7] Designation: D7566 − 19b Standard Specification for Aviation Turbine Fuel Containing Synthesized Hydrocarbons 1 n.d. 10.1520/D7566-19B.

[8] Kärcher B. Formation and radiative forcing of contrail cirrus. Nat Commun 2018;9(1).

[9] Boehm RC, Yang Z, Heyne JS. Threshold Sooting Index of Sustainable Aviation Fuel Candidates from Composition Input Alone: Progress toward Uncertainty Quantification. Energy Fuels 2022;36(4):1916–28.

[10] Kosir S, Heyne J, Graham J. A machine learning framework for drop-in volume swell characteristics of sustainable aviation fuel. Fuel 2020;274:117832.

[11] Romanczyk M, Ramirez Velasco JH, Xu L, Vozka P, Dissanayake P, Wehde KE, et al. The capability of organic compounds to swell acrylonitrile butadiene O-rings and their effects on O-ring mechanical properties. Fuel 2019;238:483–92.

[12] Edwards T. Reference jet fuels for combustion testing. In: AIAA SciTech Forum - 55th AIAA Aerospace Sciences Meeting; 2017. https://doi.org/10.2514/6.2017-0146.

[13] Vozka P, Kilaz G. A review of aviation turbine fuel chemical composition-property relations. Fuel 2020;268:117391.

[14] Vozka P, Modereger BA, Park AC, Zhang WTJ, Trice RW, Kenttämaa HI, et al. Jet fuel density via GC × GC-FID. Fuel 2019;235:1052–60.

[15] Wang Yu, Ding Y, Wei W, Cao Yi, Davidson DF, Hanson RK. On estimating physical and chemical properties of hydrocarbon fuels using mid-infrared FTIR spectra and regularized linear models. Fuel 2019;255:115715.

[16] Yang Z, Kosir S, Stachler R, Shafer L, Anderson C, Heyne JS. A GC × GC Tier α combustor operability prescreening method for sustainable aviation fuel candidates. Fuel 2021;292. https://doi.org/10.1016/j.fuel.2021.120345.

[17] Boehm RC, Yang Z, Bell DC, Feldhausen J, Heyne JS. Lower heating value of jet fuel from hydrocarbon class concentration data and thermo-chemical reference data: An uncertainty quantification. Fuel 2022;311:122542.

[18] Heyne J, Bell D, Feldhausen J, Yang Z, Boehm R. Towards fuel composition and properties from Two-dimensional gas chromatography with flame ionization and vacuum ultraviolet spectroscopy. Fuel 2022;312:122709. https://doi.org/10.1016/J.FUEL.2021.122709.

[19] Wang Yu, Wei W, Zhang Y, Hanson RK. A new strategy of characterizing hydrocarbon fuels using FTIR spectra and generalized linear model with grouped-Lasso regularization. Fuel 2021;287:119419.

[20] Striebich RC, Shafer LM, Adams RK, West ZJ, DeWitt MJ, Zabarnick S. Hydrocarbon group-type analysis of petroleum-derived and synthetic fuels using two-dimensional gas chromatography. Energy Fuels 2014;28:5696–706. https://doi.org/10.1021/ef500813x.

[21] Schug KA, Sawicki I, Carlton DD, Fan H, McNair HM, Nimmo JP, et al. Vacuum ultraviolet detector for gas chromatography. Anal Chem 2014;86(16):8329–35.

[22] Roberson ZR, Gordon HC, Goodpaster J, v.. Instrumental and chemometric analysis of opiates via gas chromatography–vacuum ultraviolet spectrophotometry (GC-VUV). Anal Bioanal Chem 2020;412:1123–8. https://doi.org/10.1007/s00216-019-02337-5.

[23] Kranenburg RF, Lukken CK, Schoenmakers PJ, van Asten AC. Spotting isomer mixtures in forensic illicit drug casework with GC–VUV using automated coelution detection and spectral deconvolution. J Chromatogr B 2021;1173:122675.

[24] Skultety L, Frycak P, Qiu C, Smuts J, Shear-Laude L, Lemr K, et al. Resolution of isomeric new designer stimulants using gas chromatography – Vacuum ultraviolet spectroscopy and theoretical computations. Anal Chim Acta 2017;971:55–67.

[25] Walsh P, Garbalena M, Schug KA. Rapid Analysis and Time Interval Deconvolution for Comprehensive Fuel Compound Group Classification and Speciation Using Gas Chromatography-Vacuum Ultraviolet Spectroscopy. Anal Chem 2016;88:11130–8. https://doi.org/10.1021/acs.analchem.6b03226.

[26] Wang FCY. Comprehensive Two-Dimensional Gas Chromatography Hyphenated with a Vacuum Ultraviolet Spectrometer to Analyze Diesel-A Three-Dimensional Separation (GC × GC × VUV) Approach. Energy Fuels 2020;34:8012–7. https://doi.org/10.1021/acs.energyfuels.0c00688.

[27] Colket M, Heyne J, Rumizen M, Gupta M, Edwards T, Roquemore WM, et al. Overview of the national jet fuels combustion program. AIAA Journal 2017;55(4):1087–104.

[28] Berrier KL, Freye CE, Billingsley MC, Synovec RE. Predictive Modeling of Aerospace Fuel Properties Using Comprehensive Two-Dimensional Gas Chromatography with Time-Of-Flight Mass Spectrometry and Partial Least Squares Analysis. Energy Fuels 2020;34:4084–94. https://doi.org/10.1021/ACS.ENERGYFUELS.9B04108/SUPPL_FILE/EF9B04108_SI_001.PDF.

[29] Boehm RC, Scholla LC, Heyne JS. Sustainable alternative fuel effects on energy consumption of jet engines. Fuel 2021;304:121378.

[30] Hall C, Rauch B, Bauder U, le Clercq P, Aigner M. Predictive Capability Assessment of Probabilistic Machine Learning Models for Density Prediction of Conventional and Synthetic Jet Fuels. Energy Fuels 2021;35:2520–30. https://doi.org/10.1021/acs.energyfuels.0c03779.

[31] Heyne JS, Colket M, Gupta M, Jardines A, Moder J, Edwards JT, et al. Year 2 of the national jet fuels combustion program: Moving towards a streamlined alternative jet fuels qualification and certification process. AIAA SciTech Forum - 55th AIAA Aerospace Sciences Meeting 2017. 10.2514/6.2017-0145.

[32] Heyne JS, Peiffer E, Colket M, Moder J, Edwards JT, Roquemore WM, et al. Year 3 of the national jet fuels combustion program: Practical and scientific impacts. AIAA Aerospace Sciences Meeting 2018 2018.. https://doi.org/10.2514/6.2018-1619.

[33] Lelevic A, Souchon V, Geantet C, Lorentz C, Moreaud M. Advanced data preprocessing for comprehensive two-dimensional gas chromatography with vacuum ultraviolet spectroscopy detection. J Sep Sci 2021;44:4141–50. https://doi.org/10.1002/jssc.202100528.

[34] Vozka P, Kilaz G. How to obtain a detailed chemical composition for middle distillates via GC × GC-FID without the need of GC × GC-TOF/MS. Fuel 2019;247:368–77. https://doi.org/10.1016/j.fuel.2019.03.009.

[35] Striebich R, Shafer L, West Z, Zabarnick S. UDR-TR-2021-159 Alternative Jet Fuel Evaluation and Specification. Dayton: 2021.

[36] Faulhaber C, Kosir ST, Borland C, Gawelek K, Boehm R, Heyne JS. Optical Dilatometry Measurements for the Quantification of Sustainable Aviation Fuel Materials Compatibility. n.d.

[37] Kroenlein K, Muzny C, Diky V, Chirico R, Magee J, Abdulagatov I, et al. NIST/TRC Web Thermo Tables (WTT) NIST Standard Reference Subscription Database 2 - Lite Edition Version 2 2011.

[38] Lelevic A, Geantet C, Moreaud M, Lorentz C, Souchon V. Quantitative Analysis of Hydrocarbons in Gas Oils by Two-Dimensional Comprehensive Gas Chromatography with Vacuum Ultraviolet Detection. Energy Fuels 2021;35:13766–75. https://doi.org/10.1021/ACS.ENERGYFUELS.1C01910.

[39] Designation: D341 − 17 Standard Practice for Viscosity-Temperature Charts for Liquid Petroleum Products 1 n.d. 10.1520/D0341-17.

[40] Colket M, Heyne J, Lieuwen TC, editors. Fuel Effects on Operability of Aircraft Gas Turbine Combustors. Reston, VA: American Institute of Aeronautics and Astronautics, Inc.; 2021.

[41] Hendershott T, Stouffer S, Monfort J, Diemer J, Busby K, Corporan E, et al. Ignition of conventional and alternative fuels at low temperatures in a single-cup swirl-stabilized combustor. AIAA Aerospace Sciences Meeting 2018 2018.. https://doi.org/10.2514/6.2018-1422.

Technical Report Documentation Page

1. Report No.	2. Government Accession No.	3. Recipient's Catalog No.
j.fuel.2022.125002		

4. Title and Subtitle	5. Report Date
Synthetic aromatic kerosene property prediction improvements with isomer specific characterization via GCxGC and vacuum ultraviolet spectroscopy	July 2022
	6. Performing Organization Code

7. Author(s)	8. Performing Organization Report No.
John Feldhausen, David C. Bell, Zhibin Yang, Conor Faulhaber, Randall Boehm, Joshua Heyne	

9. Performing Organization Name and Address	10. Work Unit No. (TRAIS)
Center of Excellence for: Alternative Jet Fuels and Environment University of Dayton, Dayton, OH 45469-0238, USA	11. Contract or Grant No. 13-C-AJFF-UD-026

12. Sponsoring Agency Name and Address	13. Type of Report and Period Covered
Federal Aviation Administration Office of Environment and Energy	Journal Article
	14. Sponsoring Agency Code

15. Supplementary Notes

16. Abstract

This research explores an advanced method of fuel composition determination and builds upon typical hydrocarbon group type analyses performed with two-dimensional gas chromatography (GCxGC). In this study, structural information of individual species within Virent's Synthetic Aromatic Kerosene (SAK) is identified by vacuum ultraviolet (VUV) spectroscopy. By mass, 71.3% of the components elute within six peaks of the chromatogram, from which 12 unique species are identified through a novel deconvolution method. Overall, the identification of 93.6%m across 26 structural isomers is made by the methods described in this work. With 93.6%m ascribed to specific isomers, the precision of fuel property predictions improves dramatically. For example, the absolute error of the viscosity prediction is reduced by 90% because of this advancement in diagnostic capability, and its 95-percentile confidence interval (precision only) is reduced by 93%. Additionally, the properties of SAK, blended with hydro processed esters fatty acids (HEFA), are demonstrated to have blended properties consistent with conventional jet fuel.

17. Key Words	18. Distribution Statement
Synthetic aromatic kerosene (SAK), Vacuum ultraviolet spectroscopy (VUV), Property predictions, Isomer identification, Deconvolution, ASCENT	

19. Security Classif. (of this report)	20. Security Classif. (of this page)	21. No. of Pages	22. Price
Unclassified	Unclassified		